*Journal of Machine Engineering, 2026, Vol. 26*
*ISSN 1895-7595 (Print) ISSN 2391-8071 (Online)*

Received*: 20 April 2026* / Accepted: *15 June 2026* / Published online: *26 September 2026*

*envelope,*
*contact line,*
*disc tool,*
*undercutting*

Long HOANG[1*]

# A NEW CAD METHOD FOR CREATING DISC TOOLS MACHINING COMPLEX HELICAL SURFACES, AVOIDING UNDERCUT AND SECOND ENVELOPE

This paper presents a detailed new CAD method for automatically determining the contact line between the machined helical surface and its disc tool, thereby creating the disc tool's primary surface. This method solves the kinematic meshing equations for the helical surface and the disc tool in cross-sections perpendicular to the disc tool axis. The method is implemented by developing a Visual Lisp program running in AutoCAD, leveraging powerful geometric functions to create cross-sections, interpolate spline curves, and easily and accurately determine the curve's normal vector, without requiring knowledge of the surface equation parameters. Verification results in the cases of the disc tools used to machine the air compressor female rotor and involute spur gear confirm the main advantages of the method, such as: The surface deviation between the disc tool created by the proposed method and the method using the normal projection in CATIA is less than 0.005 mm, and in particular, it is possible to detect and fix undercutting and double enveloping phenomena automatically.

## 1. INTRODUCTION

In mass production, one of the best practical methods for machining helical surfaces, such as helical gears and air compressor rotors, is milling or grinding with disc tools. Designing new optimal profiles of helical gears and their tools is a crucial problem in mechanical engineering. The key to the issue is that the surfaces of each kinematic pair of gears, or of a gear and its cutting tool, must envelope each other during their relative motion, and this has been presented very systematically and rigorously by Litvin [1] and Stosic [2] through the contact line meshing equations of the kinematic pair. Works that use purely analytical methods to address the issue are suitable for surfaces represented by simple, explicit mathematical equations, such as the involute, arc, and cycloid [1, 2]. Besides, A series of research studies has created new tooth profiles that are more efficient than the traditional involute profile. Lei Liu et al. [3] proposed a tooth profile design method based on controlling the relative curvature of the meshing tooth profiles. The constant relative curvature of the

[1] School of Mechanical Engineering, Hanoi University of Science and Technology, Vietnam
[*] E-mail: long.hoang@hust.edu.vn
https://doi.org/10.36897/jme/224615

meshing tooth profiles enhances the contact strength of the tooth surface and reduces the uneven distribution of contact stress. Jian Wang et al. [4] proposed a method for designing gear tooth profiles using a parabolic curve as the action curve. The proposed design method is more flexible for controlling the tooth profile shape by varying the parabola parameters. The contact and bending stresses in the new profile gears are lower than those in the traditional involute gear drive. Shu Cao et al. [5] proposed a method using B-spline curves for rotor profile design in twin-screw compressors to improve air compression efficiency. The reverse engineering of helical gears also generates 3D NURBS surface models without the original equations [6]. To accommodate such diverse helical surface forms, numerous studies have proposed methods for determining disk tools for them, as presented in the works below.

Many authors have proposed numerical methods for the meshing equation of the contact line in the kinematic pair, thereby generating the profile of a gear or cutting tool or evaluating the influence of the disc tool position on machining accuracy. More specifically, Stoic N. [7] developed the meshing equation for the helical gear and disc tool in both forward and reverse modes, provided a numerical solution method, and calculated the material distribution during the roughing step, achieving uniform wear of the disc tool during the grinding of the screw compressor rotor. Using a similar method, Stoic N. [8] determined the influence of tool setting parameters, including the angular misalignment between the tool and the rotor axis, the centre distance between the rotor and its tool, and the axis position of the tool, to correct the machining surface deviations due to tool deformation and wear. Yuwen Sun et al. [9] proposed a digital method to address various issues associated with forward and inverse calculations in grinding helical surfaces. The major difference between the proposed method and purely analytical methods is that the helical surface normal vector at the contact points must intersect the disc tool axis, which is approximately searched by the bisection method. Yan Li et al. [10] proposed a method for searching the optimal disc tool position after solving the transcendental equation of the contact line between a disc tool and a helical gear tooth surface to achieve the best disc tool profile. Po Hu et al. [11] proposed a general numerical method suited to rotors whose tooth profiles are represented by discrete points. By searching for the minimum-distance point, the proposed method avoids solving the complex nonlinear contact equation. L.V. Mohan et al. [12] presented 3D CAD-based approaches that employ Boolean operators for designing disc tools. The methods are based on a novel idea that mimics physical enveloping processes, such as material cutting, so the surface need not be regular or free of singular points. However, this method is time-consuming and has low accuracy. These methods are universal for all complex helical surface profiles. Nikola Stosic et al. [13] reported a Boolean approach, named DDS (Direct digital simulation), for generating screw compressor rotors and their tools. Guochao Li et al. [14] proposed a Boolean method for simulating the grinding of grooves on end mills. Using Boolean operations, the contact lines between the grinding wheel and the groove are illustrated and calculated to optimise the groove-grinding process. In the works [15,16], the authors use the normal projection command in CATIA to project the disc tool axis onto the gear helical surface, thereby specifying the characteristic curve of the disc tool.

From a methodological standpoint, the meshing equations for the kinematic pairs can be solved analytically, numerically, using 3D CAD Boolean operators, or via the normal projection command. Each method is designed to serve a specific purpose and circumstance, as mentioned above. This paper aims to develop a CAD method to determine the contact line between the machined helical surface and its disc tool, thereby creating the 3D disc tool model. The proposed method is oriented to give the following advantages:

- The machined helical surface is given as a 3D model without needing to know the descriptive equation parameters,
- Can evaluate and fix the undercut and double-envelope phenomena,
- Geometric input and output data are standard for all CAD/CAM/CAE systems,
- Not overly complex to apply to create automated design support tools.
- Achieves high accuracy.

## 2. PROPOSED METHOD

According to enveloping theory [1, 2], the envelope of a family of cutter surfaces during relative motion with respect to the workpiece generates the machined surface, and vice versa. An implicit equation represents the family of surfaces as

$$F(x,y,z,\theta) = 0 \tag{1}$$

where $x$, $y$, $z$ are the coordinates of a point on the surface, and $\theta$ is the movement parameter.

The intersection of the infinitesimally close surface pair can be determined by the system of equations below.

$$\begin{aligned} &F(x,y,z,\theta) = 0 \\ &F(x,y,z,\theta + \varepsilon) = 0 \end{aligned} \tag{2}$$

When $\varepsilon$ is infinitesimally small, the intersection becomes the contact line, called the characteristic curve. These limiting intersections form the envelope.

The characteristic curve is also traditionally found by the equations given below:

$$\begin{aligned} &F(x,y,z,\theta) = 0 \\ &\partial F/\partial\theta = 0 \end{aligned} \tag{3}$$

Equation 3 is called the meshing equation. Another interpretation in the parametric vector kinematics form [12] is as follows:

$$r(u,v,t) = 0 \tag{4}$$

$$\vec{N}.\vec{V} = 0 \tag{5}$$

where r is the position vector of the contact point,

$$\vec{V} = \partial r/\partial t \tag{6}$$

$$\vec{N} = \frac{\left(\frac{\partial r}{\partial u}\right)\times\left(\frac{\partial r}{\partial v}\right)}{\left\|\left(\frac{\partial r}{\partial u}\right)\times\left(\frac{\partial r}{\partial v}\right)\right\|} \tag{7}$$

Analysis of equation 5: The relative motion of the disc tool with respect to the machined helical surface includes the helical motion and rotational motion around its axis. However, the helical motion is a self-sliding motion on the helical surface, so it is ignored when solving equation 5. This leads to the condition that the normal at the contact point must intersect the axis of rotation, resulting in the characteristic curve being the normal projection of the disc tool axis onto the screw surface, as applied in works [8, 9] in CATIA, but with disadvantages that will be discussed in the discussion. In this work, equation 5 is evaluated in cross-sections perpendicular to the tool axis, which implies that the normal to the cross-section at the contact point must intersect the axis of rotation at the point where the axis and the cutting plane meet. This analysis leads to equation 8 below.

$$\vec{\mathrm{T}} \cdot \overrightarrow{\mathrm{PtPi}} = 0 \tag{8}$$

Where T is the tangent vector of the cross-section at the contact point Pt, and Pi is the intersection point of the axis and the cutting plane. Equation 8 indicates that the dot product of the tangent vector and the vector PtPi is zero, meaning that these two vectors are perpendicular to each other. The search for such a point Pt is performed by interpolating points on the cross-section to find the segment containing the contact point, and then finding the exact solution using Newton's iterative method, as shown in the algorithm flowchart below.

Figure 1 uses the following notation*:* *Na* is the number of cross-sections perpendicular to the disk axis on which the contact point will be determined; the larger *Na* is, the higher the tool accuracy.

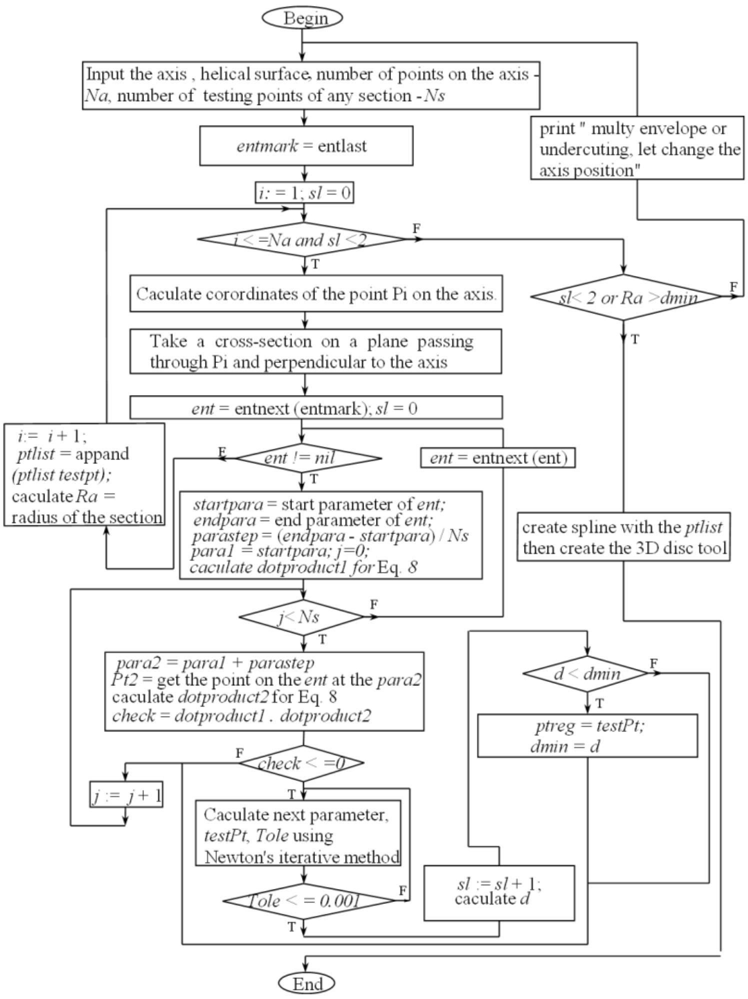


Fig. 1. Algorithm flow chart for creating the characteristic curve and the disc tool

*Ns* is the number of interpolation points on the cross-section to find the segment containing a single contact point; entlast is the last object drawn. *Sl* is the number of points that satisfy equation 8 in the cross-section under consideration; if *sl* > 1, the loop will stop and display “multiple envelope” because this will result in the entire helical surface not being machined. *Ent* is a curved segment on the cross-section; *startpara* and *endpara* are the start and end parameters of the curved segment obtained by the corresponding Visual Lisp functions. *dotproduct1* and *dotproduct2* are the dot products of the two vectors in equation 8, evaluated at two adjacent interpolation points; check is the product of these two dot products. If this product is less than 0, then between the two points lies a point satisfying equation 8 found by the Newton iterative method with a tolerance less than 0.001. *D* is the distance from the point satisfying equation 8 to the disc axis. The next step is to check whether that point is already the closest; if so, add it to the list of points on the characteristic curve. *Ra* is the radius of the cross-section at the contact point. If *Ra* is smaller than the distance from the point to the disc axis, undercutting will occur, and the disc axis position needs to be adjusted. Interpolation points on a curve by using the Visual Lisp function vlax-curve-getPointAtParam, determine the tangent vector in equation 8 by using the Visual Lisp function vlax-curve-getFirstDeriv, and calculate the radius of the section by using the Visual Lisp functions vlax-curve-getFirstDeriv and vlax-curve-getSecondDeriv.

## 3. VERIFICATION RESULT AND DISCUSSION

### 3.1. VERIFICATION RESULT FOR AIR COMPRESSOR ROTOR DISC TOOL PROFILING

To verify the proposed method, an AutoLISP program was implemented based on the algorithm flowchart shown above. The program was run with input data consisting of a 3D rotor model of the air compressor obtained from reverse engineering. Figures 2 and 3 show the results when the tool axis is mispositioned.

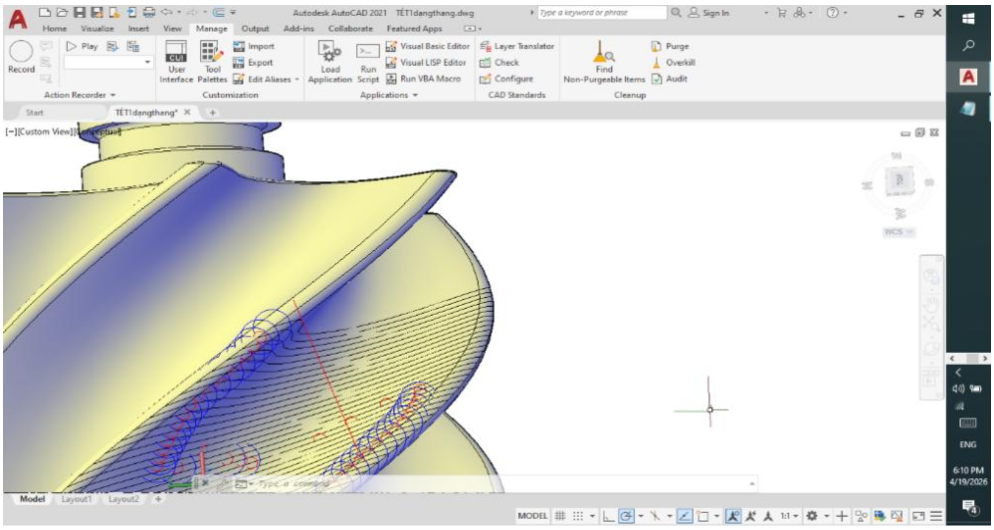

Fig. 2. Multiple envelope phenomena

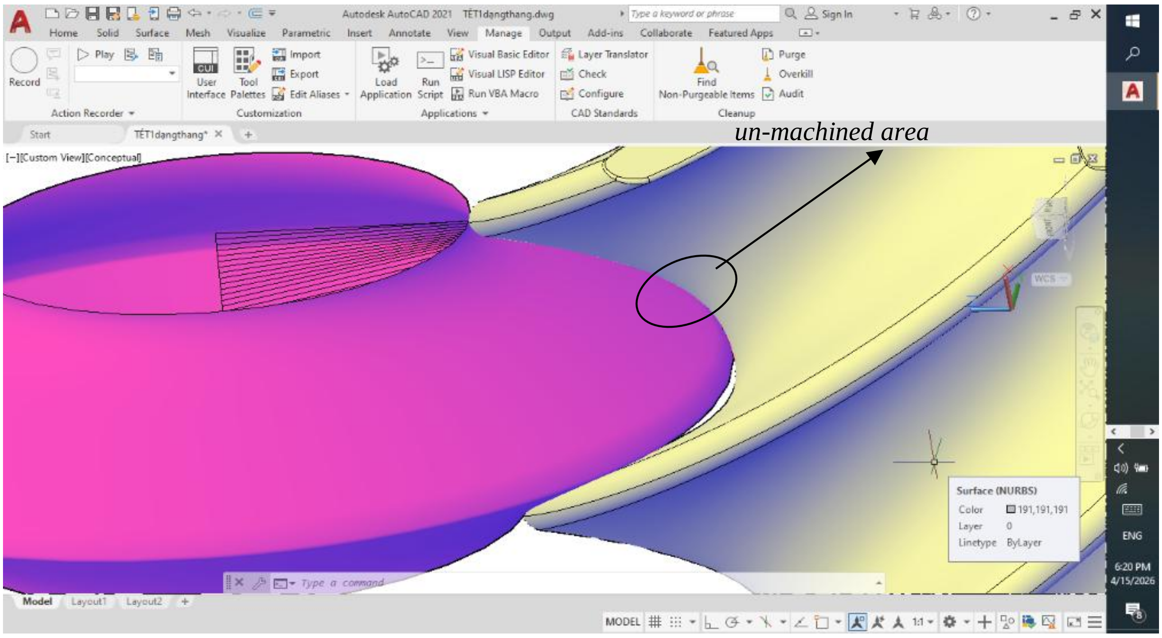


Fig. 3. The disc tool cannot machine the whole helical surface

In Figure 4, every small circle has a larger circle concentric with it, meaning that on each cross-section, there exists only one point satisfying the meshing equation, and that point is the closest. This means that the tool generated from the characteristic curve passing through the closest points can machine the entire surface, as shown in Fig. 5.

Two 3D models of the disc tool, created using the proposed method and the projection method in CATIA, were compared using Geomagic Control X. The deviations are very small, as shown in Fig. 6 and 7 and in Table 1.

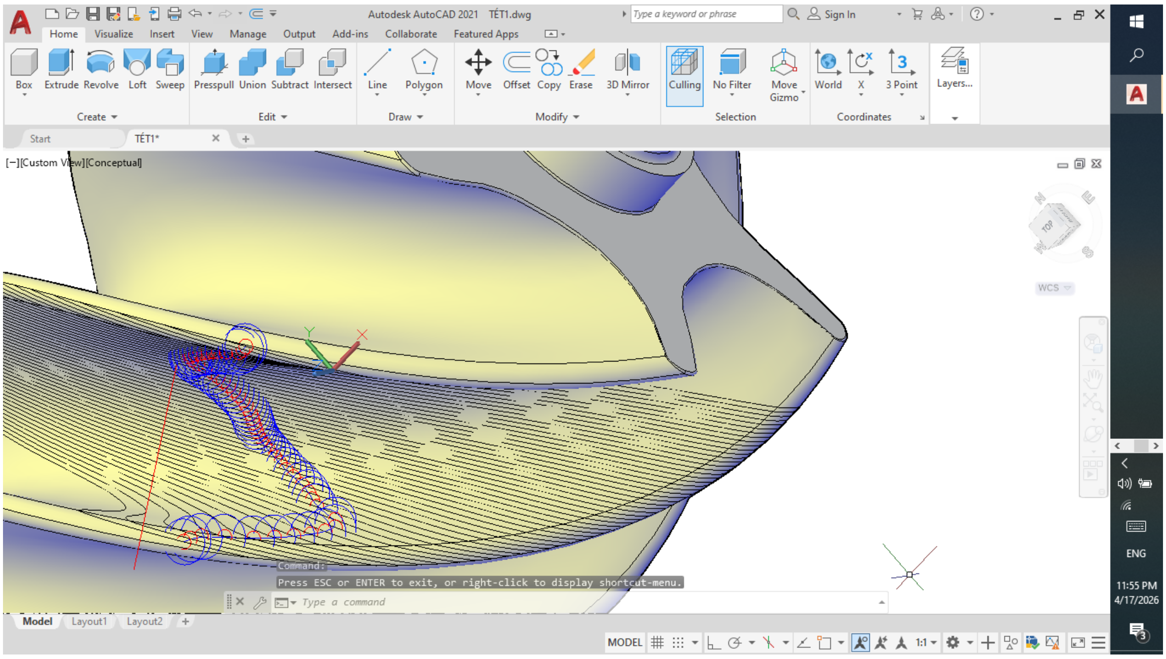

Fig. 4. The multiple envelope phenomenon did not occur

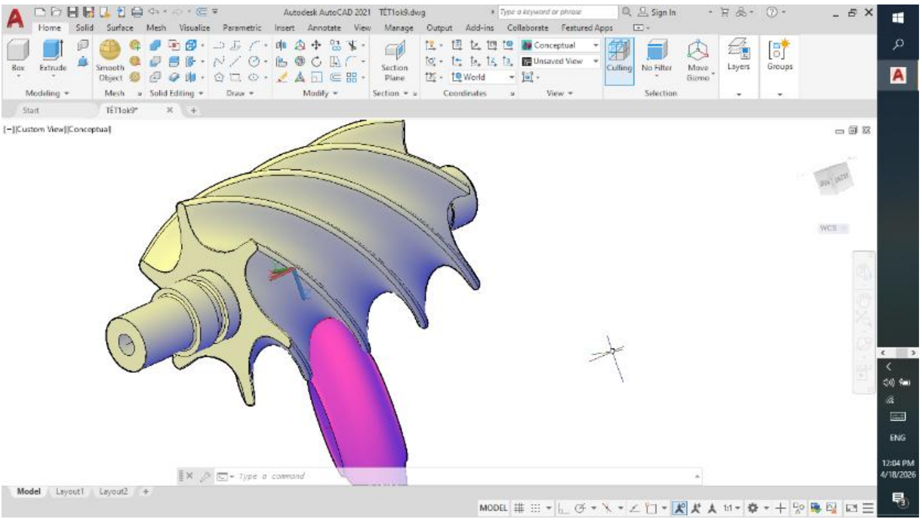

Fig. 5. The disc tool can machine the entire helical surface

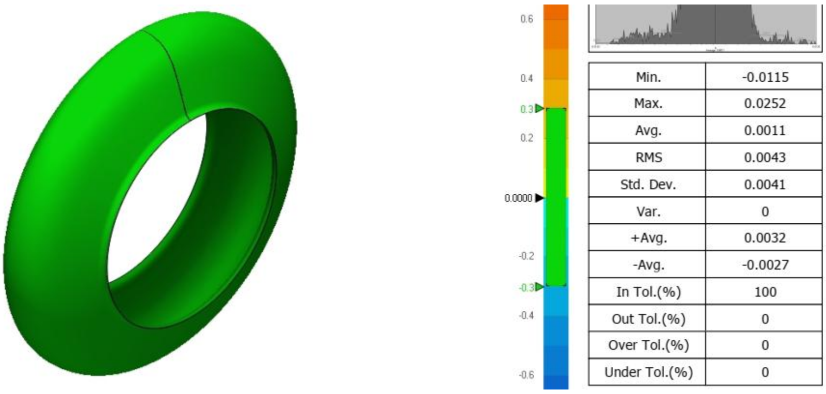


| | |
|---|---|
| Min. | -0.0115 |
| Max. | 0.0252 |
| Avg. | 0.0011 |
| RMS | 0.0043 |
| Std. Dev. | 0.0041 |
| Var. | 0 |
| +Avg. | 0.0032 |
| -Avg. | -0.0027 |
| In Tol.(%) | 100 |
| Out Tol.(%) | 0 |
| Over Tol.(%) | 0 |
| Under Tol.(%) | 0 |

Fig. 6. 3D deviation of the disc tools created by the two methods

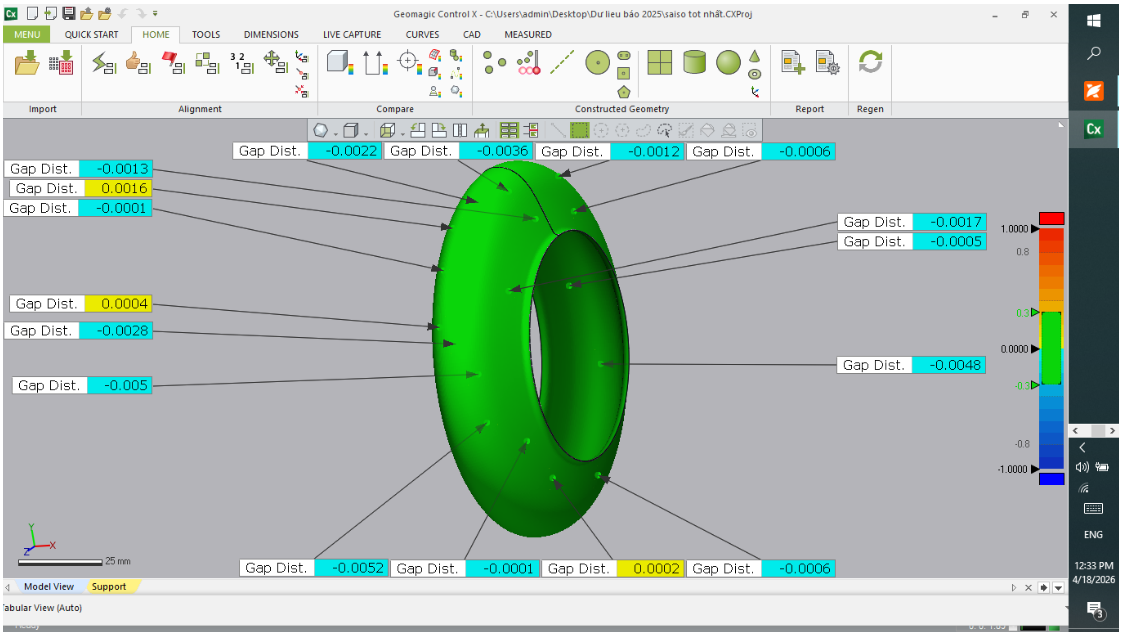


Fig. 7. 3D point deviation of the disc tools created by the two methods

Table 1. 3D point deviation of the disc tools created by the two methods (in mm).

| Name | Reference Pos. | | | Measured Pos. | | | Gap Dist. |
|---|---|---|---|---|---|---|---|
| | X | Y | Z | X | Y | Z | |
| CMP1: 1 | 24.9973 | -165.002 | -24.4782 | 24.9964 | -165.003 | -24.4778 | -0.0012 |
| CMP1: 2 | 24.9979 | -160.002 | 10.6666 | 24.9951 | -160.004 | 10.6662 | -0.0036 |
| CMP1: 3 | 19.9991 | -160.003 | 21.8783 | 19.9985 | -160.005 | 21.8775 | -0.0022 |
| CMP1: 4 | 15.0014 | -165.004 | 31.4575 | 15.0009 | -165.003 | 31.4584 | 0.0016 |
| CMP1: 5 | 15.0017 | -175.004 | 42.5471 | 15.0018 | -175.004 | 42.547 | -0.0001 |
| CMP1: 6 | 15.0017 | -190.002 | 51.6373 | 15.0016 | -190.002 | 51.6377 | 0.0004 |
| CMP1: 7 | 19.999 | -195.001 | 53.1644 | 19.9982 | -195.002 | 53.1618 | -0.0028 |
| CMP1: 8 | 24.998 | -205 | 51.7941 | 24.9941 | -205.001 | 51.7909 | -0.005 |
| CMP1: 9 | 24.997 | -220 | 51.37 | 24.9929 | -219.999 | 51.3668 | -0.0052 |
| CMP1: 10 | 29.9992 | -230 | 36.9027 | 29.999 | -230 | 36.9026 | -0.0001 |
| CMP1: 11 | 29.9991 | -245 | 23.836 | 29.9994 | -245 | 23.836 | 0.0002 |
| CMP1: 12 | 29.683 | -252.741 | -7.6731 | 29.6824 | -252.741 | -7.6731 | -0.0006 |
| CMP1: 13 | 15.0014 | -229.998 | -52.4411 | 15.0027 | -229.997 | -52.4368 | -0.0048 |
| CMP1: 14 | 10.0022 | -205 | -50.1963 | 10.0026 | -205 | -50.1961 | -0.0005 |
| CMP1: 15 | 29.9993 | -185 | 32.2925 | 29.9977 | -185.001 | 32.2921 | -0.0017 |
| CMP1: 16 | 29.9993 | -170 | 6.0398 | 29.9981 | -170.001 | 6.0398 | -0.0013 |
| CMP1: 17 | 29.9993 | -175 | -20.5407 | 29.9987 | -175 | -20.5406 | -0.0006 |
| Min. | 10.0022 | -252.741 | -52.4411 | 10.0026 | -252.741 | -52.4368 | -0.0052 |
| Max. | 29.9993 | -160.002 | 53.1644 | 29.9994 | -160.004 | 53.1618 | 0.0016 |

### 3.2. VERIFICATION RESULT FOR INVOLUTE SPUR GEAR DISC TOOL PROFILING

Use SolidWorks to create the involute spur gear as shown in Fig. 8.

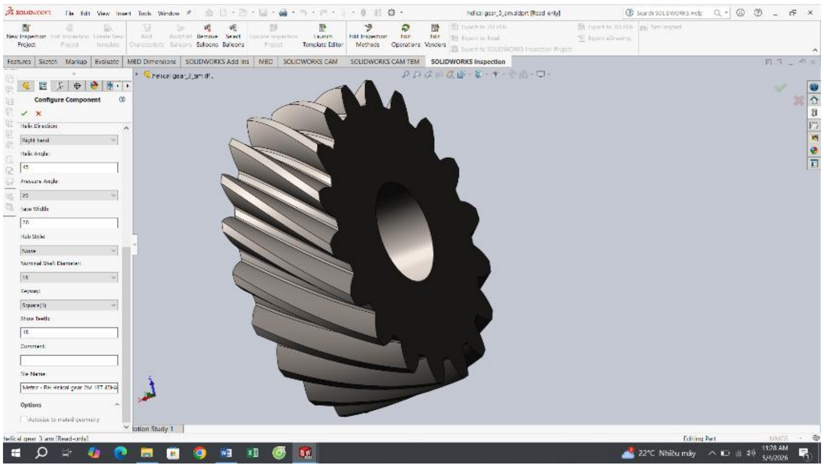

Fig. 8. Involute spur gears are created in SolidWorks

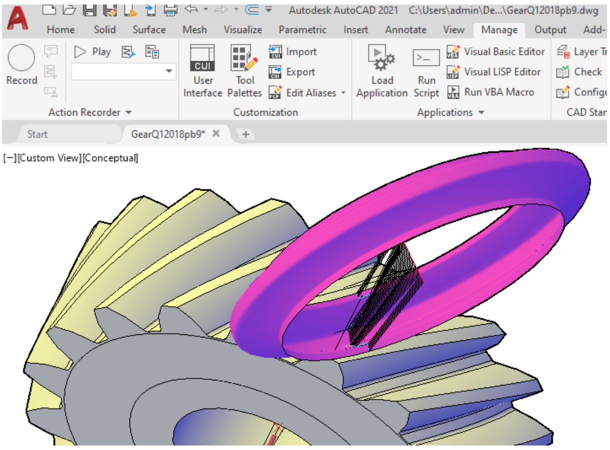


Fig. 9. The disc tool is created without any undercutting

The disc tool is created without any undercutting, as shown in Fig. 9. Two 3D models of the disc tool, created using the proposed method and the projection method in CATIA, were compared using Geomagic Control X. The deviations are very small, as shown in Figs. 10 and 11 and in Table 2.

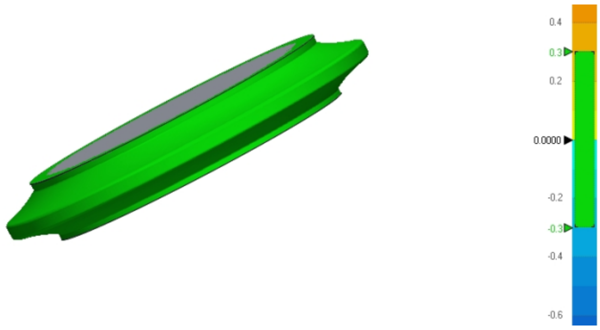


| | |
|---|---|
| Min. | -0.023 |
| Max. | 0.025 |
| Avg. | -0.0002 |
| RMS | 0.0109 |
| Std. Dev. | 0.0109 |
| Var. | 0.0001 |
| +Avg. | 0.009 |
| -Avg. | -0.009 |
| In Tol.(%) | 100 |
| Out Tol.(%) | 0 |
| Over Tol.(%) | 0 |
| Under Tol.(%) | 0 |

Fig. 10. 3D deviation of the disc tools created by the two methods

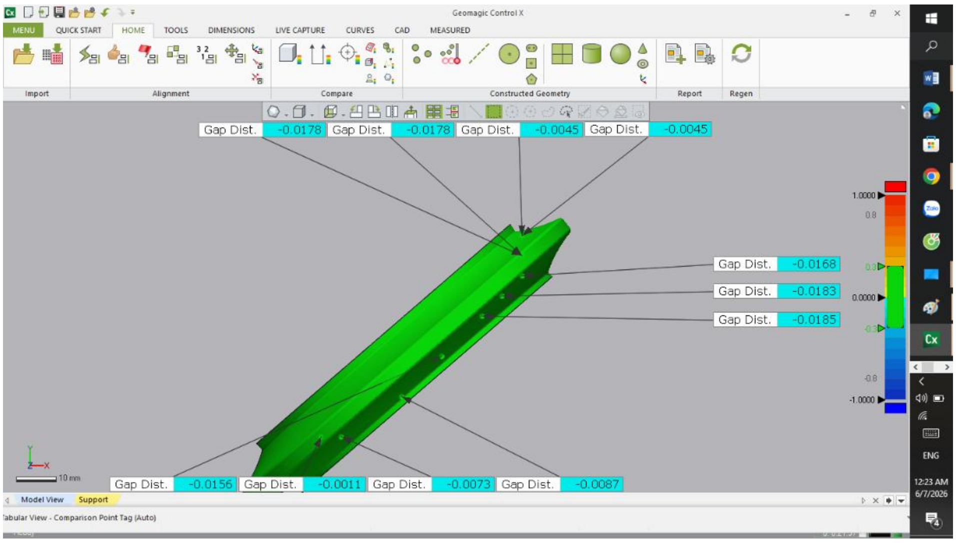


Fig. 11. 3D point deviation of the disc tools created by the two methods

The proposed method is quite similar to the “min distance” method [11]. Still, it differs in that it finds all points that satisfy the meshing equation, including the “min distance” point, and then detects the unmachined area to readjust the disk tool's axis position. This method is also quite similar to the method of normal projection of the disc axis onto the helical surface [16] but differs in that it solves the meshing equation on each cross-section, so geometrically, the contact points are the projection of the intersection point of the disc axis and the cutting plane onto the section, so it is stable, do not require an infinitely long axis when the helical surface has points where the normal is almost parallel to the disc axis. Furthermore, it can automatically determine the disc axis position, thereby avoiding undercuts or multiple-envelope phenomena. The accuracy of the proposed method can be achieved as desired by increasing the number of interpolation points.

Table 2. 3D point deviation of the disc tools created by the two methods (in mm)

| Name | Reference Pos. | | | Measured Pos. | | | Gap Dist. |
|---|---|---|---|---|---|---|---|
| | X | Y | Z | X | Y | Z | |
| CMP1: 1 | 44.9993 | 35.0027 | -94.3905 | 45.0004 | 34.9985 | -94.3912 | -0.0045 |
| CMP1: 2 | 44.9993 | 35.0027 | -94.3905 | 45.0004 | 34.9985 | -94.3912 | -0.0045 |
| CMP1: 3 | 44.9984 | 29.9989 | -74.4148 | 44.9877 | 29.9912 | -74.4268 | -0.0178 |
| CMP1: 4 | 44.9984 | 29.9989 | -74.4148 | 44.9877 | 29.9912 | -74.4268 | -0.0178 |
| CMP1: 5 | 45.0009 | 24.9992 | -74.6221 | 44.9881 | 25.0097 | -74.625 | -0.0168 |
| CMP1: 6 | 40.002 | 19.9984 | -71.0507 | 39.9882 | 20.0098 | -71.0547 | -0.0183 |
| CMP1: 7 | 35.0017 | 14.9986 | -68.5378 | 34.9881 | 15.0099 | -68.5432 | -0.0011 |
| CMP1: 8 | 25.0015 | 4.9985 | -66.4823 | 24.9915 | 5.0085 | -66.4887 | -0.0011 |
| CMP1: 9 | 14.9985 | -4.9979 | -68.468 | 14.9939 | -4.9916 | -68.4719 | -0.0011 |
| CMP1: 10 | -4.9997 | -14.9997 | -65.7015 | -4.9993 | -14.9993 | -65.7024 | -0.0011 |
| CMP1: 11 | 0.0004 | -15.0006 | -69.766 | -0.0033 | -14.9946 | -69.7678 | -0.0011 |
| Min. | -4.9997 | -15.0006 | -94.3905 | -4.9993 | -14.9993 | -94.3912 | -0.0011 |
| Max. | 45.0009 | 35.0027 | -65.7015 | 45.0004 | 34.9985 | -65.7024 | -0.0011 |

## 4. CONCLUSION

This paper presents a detailed new CAD method for automatically determining the contact line between the machined helical surface and its disc tool, thereby creating the disc tool's primary surface. The main new contribution of the proposed method is that it finds all points that satisfy the meshing equation and then detects the unmachined area to readjust the disk tool's axis position, thereby avoiding undercut. Verification results from applying the proposed method to create the disc tool used to machine the helical surface of the air compressor female rotor and the involute spur gear have confirmed the following advantages of the proposed method:

- The machined helical surface is given as a 3D model without needing to know the descriptive equation parameters,
- Can evaluate and fix the undercut and multiple envelope phenomena,

- Geometric input and output data are standard for all CAD/CAM/CAE systems,
- Not overly complex to apply to create such automated design support tools, which plug into AutoCAD.
- Achieves high accuracy, the RMS deviation is 0.001 mm.

The proposed method could serve as a basis for developing software to support the design of rotary tools for machining any helical surfaces with constant pitch, such as helical spur gears, air compressor screws, and helical grooves on end mills.

ACKNOWLEDGEMENTS

*The authors are grateful to the Ministry of Education and Training in Vietnam for financial support under project number B2026-BKA-10.*

REFERENCES

[1] LITVIN F.L., FUENTES A., 2004, *Gear Geometry and Applied Theory*, Cambridge University Press, 818.
[2] STOSIC N., SMITH I.K., KOVACEVIC A., MUJIC E, 2011, *Geometry of Screw Compressor Rotors and Their Tools*, Journal of Zhejiang University-SCIENCE A (Applied Physics & Engineering), 12/4, 31–326.
[3] LEI L., MENG F., NI J., 2019, *A Novel Non-Involute Gear Designed Based on Control of Relative Curvature*, Mechanism and Machine Theory, 140, 144–158.
[4] WANG J., HOU L., LUO S., RAY Y., WU C., 2013, *Active Design of Tooth Profiles Using Parabolic Curve as The Line of Action*, Mechanism and Machine Theory, 67, 47–63.
[5] SHU C., HE X., ZHANG R., XIAO J., SHI G., 2019, *Study on the Reverse Design of Screw Rotor Profiles Based on a B-Spline Curve*, Advances in Mechanical Engineering, 11/10, 1–17.
[6] LONG H., 2024, *A New Envelope Computational Method for Meshing Heliacal Gears Profiling Applied to Air Compressor Screw Pair*, Advances in Science and Technology Research Journal, 18/4, 347–354 https://doi.org/10.12913/22998624/189674
[7] STOIC N., 2006, *A Geometric Approach to Calculating Tool Wear in Screw Rotor Machining*, International Journal of Machine Tools & Manufacture, 46, 1961–1965.
[8] STOIC N., 2006, *Evaluating Errors in Screw Rotor Machining by Tool to Rotor Transformation*, Proc. IMechE Part B, Journal of Engineering Manufacture, 220, 1589–1596.
[9] YUWEN S., JUN W., DONGMING G., QIANG Z., 2008, *Modelling and Numerical Simulation for the Machining of Helical Surface Profiles on Cutting Tools*, Int. J. Adv. Manuf. Technol., 36, 525–534.
[10] YAN L., GANG L., ZHONGHOU W., WENMIN Z., 2024, *A Form-Grinding Wheel Optimisation Method for Helical Gears Based on a PSO-SVM Model*, Precision Engineering, 88, 664–673.
[11] HU, P.; ZHOU, J.; LI, Y., 2025, *A General Numerical Method to Calculate Cutter Profiles for Formed Milling of Helical Surfaces with Machinability Analysis*, Appl. Sci., 15, 9077, 1-17, https://doi.org/ 10.3390/app15169077
[12] MOHAN L.V., SHUNMUGAM M.S., 2004, *CAD Approach for Simulation of Generation Machining and Identification of Contact Lines*, International Journal of Machine Tools & Manufacture, 44, 717–723.
[13] STOSIC N., MUJIC E., SMITH I.K., KOVACEVIC A., 2008, *Profiling of Screw Compressor Rotors by Use of Direct Digital Simulation*, International Compressor Engineering Conference at Purdue, 1–8.
[14] GUOCHAO L., JIE S., JIANFENG L., 2014, *Process Modelling of End Mill Groove Machining Based on Boolean Method*, Int J Adv Manuf Technol, 75, 959–966.
[15] NGUYEN T.-L., HOANG L., 2021, *Disc Tool Profiling for Air Compressor Screws with Complex Characteristic Curves*, Journal of Machine Engineering, 21/3, 101-109.
[16] BERBINSCHI S., TEODOR V.G., OANCEA N., 2012, *3D Graphical Method for Profiling Tools That Generate Helical Surfaces*, Int. J. Adv. Manuf. Technol., 60, 505–512.